

# Calibration of Cosmic Watch Desktop Muon Detector: Evaluating the Effects of Atmospheric Pressure and Material Interaction on Detection Accuracy

Fanyi Shi<sup>1,#,\*</sup>, Yuwei Niu<sup>2,#</sup>, Zibing Liu<sup>3,#</sup> and Yanxin Bian<sup>4,#</sup>

<sup>1</sup> Stephenperse Foundation, Cambridge, CB2 1TN, UK, 990597@stephenperse.com

<sup>2</sup> The Masters School, New York, 10522, USA, crystalniu56@gmail.com

<sup>3</sup> Daqing Cambridge International Center, Daqing, 163712, China, lunaliu080808@163.com

<sup>4</sup> Suzhou Foreign Language School, Suzhou, 215000, China, beverlyy.bian@gmail.com

\*corresponding author

#co-first authors

## Abstract:

This study focuses on the analysis of data obtained from Cosmic Watch (CW) muon detectors. The objective is to establish a standardised procedures for the enhancement of accuracy of muon detection in varying environments. By applying correlation analysis, the linear regression line is used to addresses the impact of atmospheric pressure on muon detection rates, which is clarified in the dissertation. A significant aspect of the research involves the rectification of systematic errors, which includes inconsistencies in pressure and temporal discrepancies across groups of Cosmic Watch (CW) detectors. Furthermore, the study investigates the influence of diverse materials on muon penetration, with the detectors being covered with lead, iron, and no material, respectively. The corrected data provide more reliable detection of double- and triple-coincident events and insights into the interactions between certain material and muons. Although there are limitations, the developed calibration model provides a robust framework for future experiments involving muon detection, with potential applications in studying the properties of cosmic-ray muons, and angular distribution.

**Keywords:** Cosmic Watch, muon, calibration model, linear regression correction.

## 1. Introduction

In this research, we took the raw data from the Cosmic Watches(CW) and created a model that converts the data into a standardised, practical format. We propose to create this model to identify double and triple coincidence events and distinguish between different experimental environments. The data we are using comes from the Cosmic Watch, known as the Muon Detector. The cosmic rays[1] from space are constantly received by the Earth, which is the flux of high energy particles include mainly protons and atomic nuclei, these particles are mostly relativistic. When the cosmic rays the earth, the low-energy ones are heavily affected by the solar wind[2]we report the first sta-

tistical study of ultra-low frequency (ULF and geomagnetic field[3] and the high energy flux loses energy from the interactions with the cosmic microwave background [4]. The primary cosmic rays passing through the atmosphere interact with the oxygen or nitrogen nuclei, much of the energy during the collisions goes into the production of short-lived mesons such as pions[5] and kaons[6], where the cosmic ray muons (with half-lives of  $2.2 \times 10^{-6}$  s) originally come from. These muons, with a half-life of 2.2 microseconds, can lose energy through ionization but remain relativistic enough to potentially reach the Earth's surface before decaying if their energy exceeds 2.4 GeV. [4],[7]

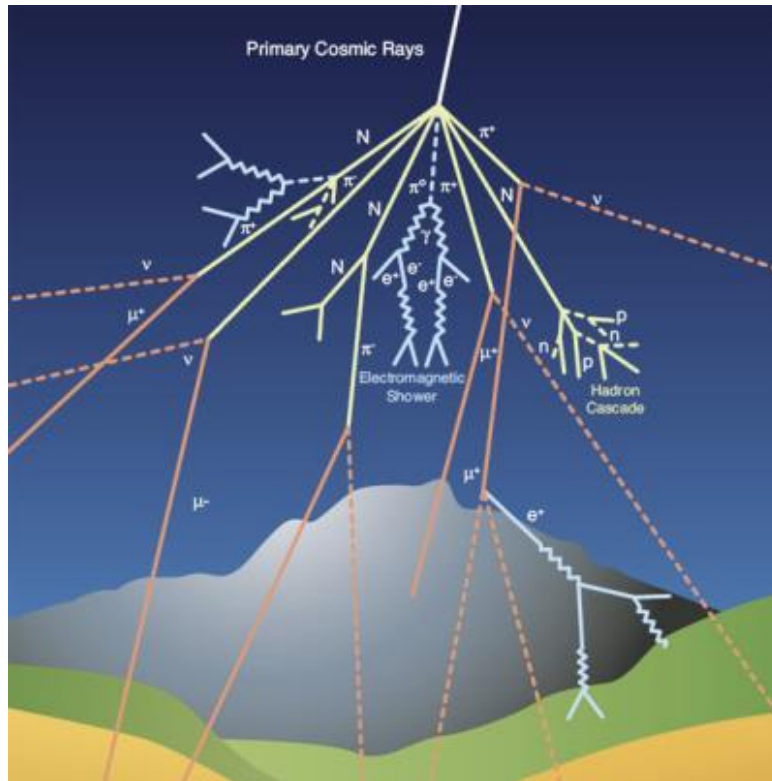


Figure1.1 decay chains of the interaction of cosmic rays with atmosphere[8]

## 2. Methodology

### 2.1 Mechanism of desktop Cosmic Watch

The cosmic watch (muon detector) is a device consisting of a silicon photomultiplier (SiPM)[9]their low density implies a weak stopping power of high energy radiations, thus a limited light output and sensitivity. To enhance their performances, polymeric scintillators can be loaded with dense nanoparticles (NPs, which is a light-sensitive component, consist of multiple microcells, each acting as a P-N junction<sup>[1]</sup>. Upon deposition of energy by a charged particle in the scintillator[10]particle physics, neutrino physics, or medical physics. An example of application for this kind of detectors are Compton polarimeters such as POLAR-2 or LEAP, for which a low-Z material is needed for the Compton effect to be dominant down to as low energy as possible. Such detectors aim to measure low energy Compton depositions which produce small amounts of optical light, and for which optimizing the instrumental optical properties consequently imperative.”,“language”:"en",“note”:"arXiv:2407.10741 [astro-ph]”,“number”:"arXiv:2407.10741”,“publisher”:"arXiv”,“source”:"arXiv.org”,“title”:"Optimizing

1 P-N junction: in semiconductor devices, P-N junction are used to control the flow of current or to convert light signals into electrical signals in detectors.

the light output of a plastic scintillator and SiPM based detector through optical characterization and simulation: A case study for POLAR-2”,“title-short”:"Optimizing the light output of a plastic scintillator and SiPM based detector through optical characterization and simulation”,“URL”:"http://arxiv.org/abs/2407.10741”,“author”:[{"family”:"De Angelis”,“given”:"Nicolas"}, {"family”:"Cadoux”,“given”:"Franck"}, {"family”:"Husi”,“given”:"Coralie"}, {"family”:"Kole”,“given”:"Merlin"}, {"family”:"Mianowski”,“given”:"Sławomir"}],“accessed”:[{"date-parts”:[["2024",8,22]]}, {"date-parts”:[["2024",7,15]]}],“schema”:"https://github.com/citation-style-language/schema/raw/master/csl-citation.json"} , a portion of this energy is subsequently re-emitted isotropically as photons. The photons, upon exciting an electron in the depletion region[11]where lithium depleted regions may develop and cause a sudden exponential drop in the cell’s terminal voltage. Having accurate predictions of performance under such conditions is necessary for electric vertical takeoff and landing (eVTOL, result in the creation of an electron-hole pair. Upon impact with the light-sensitive region of the SiPM, photons have the potential to initiate an avalanche<sup>2</sup>[12]SPDs based on In-

2 Avalanche: When a free electron is accelerated in a strong electric field, it gains enough energy to collide with other atoms, creating more free electrons, This leads to a

GaAs/InP single-photon avalanche diodes (SPADs, resulting in a Geiger discharge within the SiPM microcells and the generation of a measurable current. Each microcell functions as a photon-triggered switch, with the total cur-chain reaction in which the number of electrons rapidly increases.

rent proportional to the number of activated microcells. The resulting current is then conveyed through a bespoke printed circuit board (PCB)[13] that amplifies and shapes the signal, thereby enabling a microcontroller to ascertain the time stamp and peak voltage of the event (Axani et al., 2018; Axani, 2019).

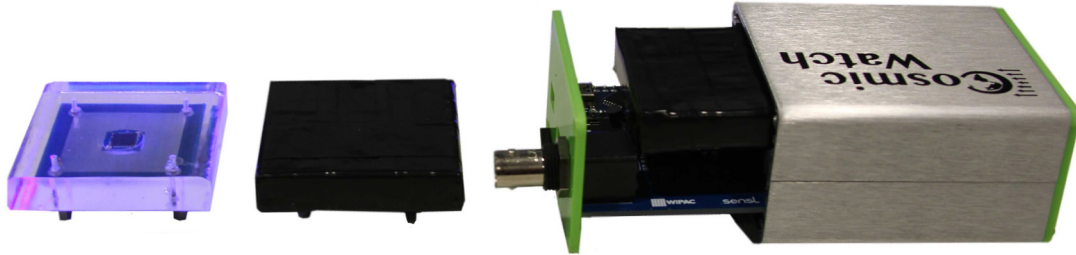


Figure2.1 the scintillator on the left with SiPM[4]

### 2.2 Formulars

The present study is concerned with the correlation between the top and bottom detector sets, as well as the correlation between different detector sets, and the variables of SiPM intensity, count rate, time stamp and coincidence. Furthermore, the detectors were covered with three different materials (no material, lead, iron) which can be identified by examining the count rate of each device, as the penetration of muons varies with the covering material. One of the key areas of focus in this study is data processing. We propose a methodology involving the reorganization of data, unification of units, calculation, and calibration to a standard value. The rationale behind this approach is that inconsistencies in conditions can lead to confusion. Once this process is complete, we will be able to compare quantities in detectors, thereby gaining valuable insights. In our study, the detectors were not initiated simultaneously and experienced different seasonal conditions, resulting in a range of air pressure readings. Additionally, the duration of each recording differed. When these two factors are considered together, it becomes evident that calculating an average pressure for each recording is not a precise approach. To effectively visualize the relationship between count rate and air pressure, we developed a code to generate graphs. Some calculations were employed in this process:

$$R_i = \frac{\sum count\ rate}{\sum timestamps / 1000 * 3600} \quad (2.2.1)$$

$$R_i = \frac{R}{\langle r \rangle} \quad (2.2.2)$$

$R$  is average rate per hour,  $\langle r \rangle$  is total average pressure  
The timestamp is divided by 1000\*3600 as it is initially represented in unit of ms

$$P_i = \frac{total\ average\ pressure}{\sum timestamps} \quad (2.2.3)$$

$$? Pressure = P_i - P_{std} \quad (2.2.4)$$

where the timestamps have unit ms which is converted into hour, total average pressure is also hourly counted.

$$Normalised\ rate = \frac{R_i}{\Delta Pressure} \quad (2.2.5)$$

Here we utilise a regression line to represent the correlation as the regression is useful for calibrate the pressure to a standard atmospheric pressure. The calculations here are separated into top and bottom detectors. Here is the specific version of the calibration:

$$\overline{\Delta Pressure} = \left[ \frac{\sum P_i - P_{std}}{n_1} + \frac{\sum P_i - P_{std}}{n_2} \right] / 2 \quad (2.2.6)$$

$$Average\ Normalised\ rate = \left[ \frac{\sum R_{n1}}{n_1} + \frac{\sum R_{n2}}{n_2} \right] / 2 \quad (2.2.7)$$

$P_i$  is a verage pressure (per hour) of events that have coincidence 1

$P_{std}$  is stand ardatmospheric pressure

$n$  is number of  $P_i$  points in the graph

To mitigate the impact of variations in air pressure on the data, the measurements were calibrated to standard pressure values. This entailed the plotting of data points on scatter plots and the application of the least squares method of linear regression to model the relationship between the independent and dependent variables. The regression analysis facilitates the standardization of measurements across disparate datasets, ensuring a consistent air pressure condition and reducing the impact of systematic errors. The regression equation is in the form of  $y = ax + b$ ,

where the slope and intercept can be calculated using the following formulas:

The formula for the slope is given by

$$\hat{b} = \frac{\sum_{i=1}^n XiYi - n\bar{x}\bar{y}}{\sum_{i=1}^n xi^2 - n(\bar{x})^2} \quad (2.2.8)$$

while the formula for the intercept is

$$\hat{a} = \bar{y} - \bar{b}\bar{x} \quad (2.2.9)$$

The correlation coefficient  $r$  is calculated using the following formula

$$r = \frac{\sum(x_i - \bar{x}) \times (y_i - \bar{y})}{\sqrt{\sum(x_i - \bar{x})^2 \times (y_i - \bar{y})^2}} \quad (2.2.10)$$

These formulas facilitate data fitting and pressure error correction using Python. The data were fitted by calculating the ratio of the impedance to the average impedance,

$\frac{Ri}{Rave}$ , and the ratio of the pressure to the average pressure,  $\frac{Pi}{Pave}$ . This allowed for the correction of pressure deviations.

To further validate the accuracy of the regression results, we employed the chi-squared test to assess the reliability of the regression coefficients  $a$  and  $b$ . The chi-squared test formula is as follows:

$$\chi^2 = \sum \frac{O_i - E_i^2}{E_i} \quad (2.2.11)$$

In this formula,  $O_i$  represents the observational data that was recorded, whereas  $E_i$  denotes the expected value that was calculated according to the entire set of data[14]

In this test, a 10% confidence level was employed to ascertain the significance of the regression coefficients. In conclusion, the chi-squared values for each group of top and bottom detectors were calculated and employed to assess the viability of detecting identical muon events with the Cosmic Watch detectors.

$$\text{Corrected rate} = (1 - \beta \times \overline{\Delta pressure}) \times \text{Average normalised rate} \\ \beta \text{ is the slope of regression line.} \quad (2.2.12)$$

The normalised rate is employed as a means of facilitating comparison across disparate conditions or datasets. This equation incorporates a linear correction to account for the

impact of pressure deviation on the normalised rate. The multiplication of  $(1 - \beta \times \overline{\Delta pressure}) \times \text{normalised rate}$  represents a form of bias correction, which aims to adjust the rate based on the influence of pressure deviations. This effectively removes or reduces the systematic errors introduced by external factors. An average of the pressure and its normalised rate for a group of upper and lower detectors was calculated.

The constant difference between the pressure measurements of the Cosmic Watch operated simultaneously was corrected for using the aforementioned equation. The data points for the Bottom Cosmic Watch were shifted to the right by the calculated value, while those for the Top Cosmic Watch were shifted to the left by the same value.

In particular, the data collected from the Cosmic Watch detectors was processed and analyzed across a range of time periods. A comparison of the data from the top and bottom detectors revealed performance differences between the detectors and variations in count rates under different pressure conditions. The results yield valuable insights into the sensitivity of the detectors and the overall performance of the system. To ascertain the veracity of the calibrated rate, it is necessary to determine the discrepancy between the mean pressure for each file in the detectors and the standard atmospheric pressure. Given that the change in pressure is inversely proportional to the change in rate, it can be expected that the change in rate will follow the path of the deviation of the atmospheric pressure. As the detectors were covered with three distinct materials: no material, lead, and iron. By comparing the variations in count rate under different covering materials, we were able to more accurately assess the effect of materials on detector performance. After correcting the data using linear regression, we were able to ascertain the trends in material impact on muon detection and further verify the stability and consistency of the detectors under various conditions

### 3. Data and Results

We identify an almost constant discrepancy between the beginning operation times of individual Cosmic Watches where we examined the particle detections of Cosmic Watches stacked together as shown in FIG. 3.1

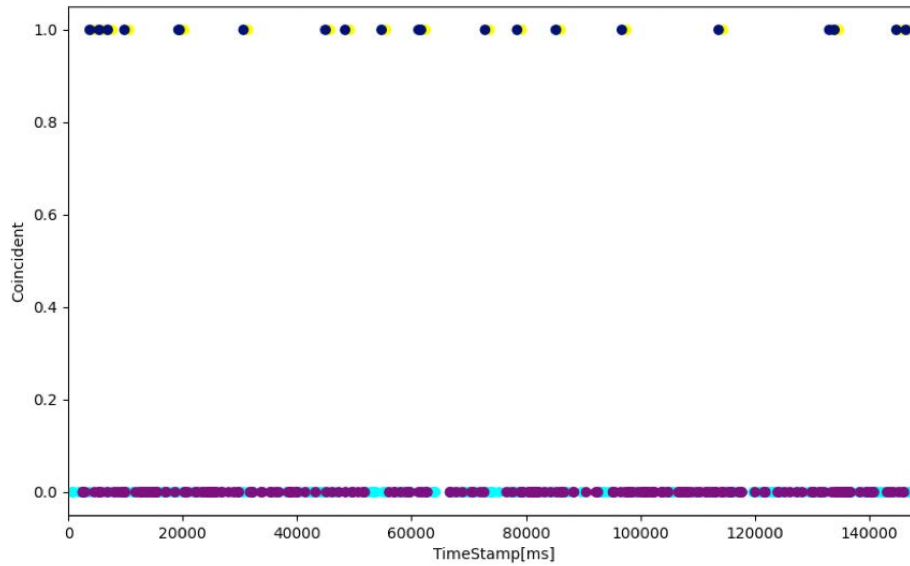


**FIG.3.1 Coincidence detection of particle events between two Cosmic Watches (B02 and T02) over time.(B02-blue:0 yellow:1,T02-purple:0 darkblue:1)**

It is unclear which of the yellow points corresponds to the blue point, so the goal is to identify the relationship between the TimeStamps of the coincident events of a pair of cosmic clocks. An important step is to use each TimeStamp of the lower cosmic clock to calculate the exact TimeStamp difference. We also added another condition, which is to calculate only the near 2000ms TimeStamps of a coincident event, because when the TimeStamps difference exceeds 2000ms, the chance of detecting the same muon decreases significantly. We plot out 3 pairs, here is

an example in FIG.3.2.

In order to assert which files of data were captured simultaneously among the various cosmic watches, we plotted a graph of average pressures versus file names. (shown in FIG. 5) This was based on the assumption that the data obtained at the same time exhibited a near-equivalent average air pressure. This will facilitate more accurate computation of the aforementioned correlation function graphs. For instance, B02FileC001.txt and B45FileC001.txt were recorded at the same time.

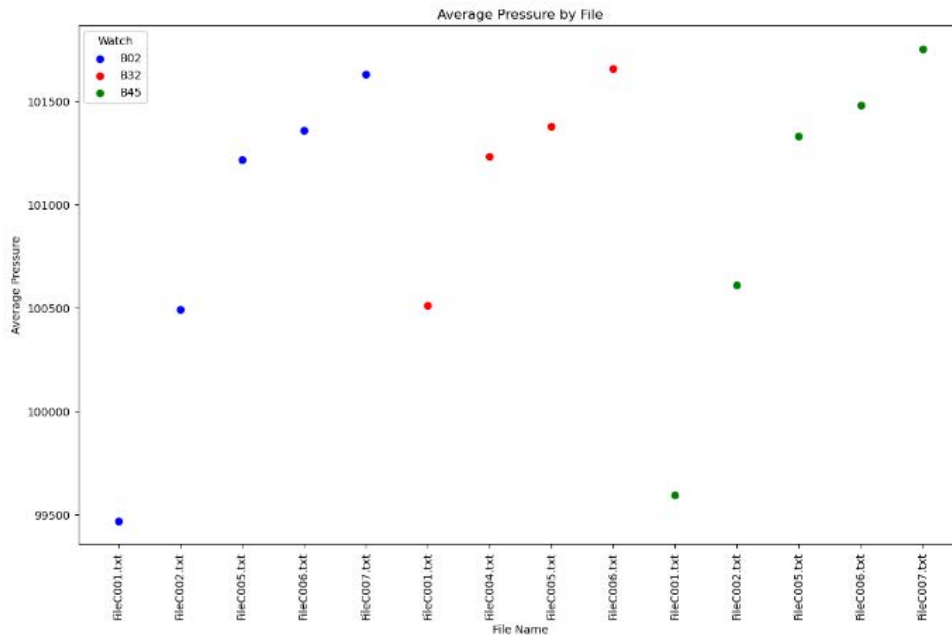


**FIG.3.3 Average air pressure of files verses file names**

To further verify the results obtained through the above method, we plotted TimeStamp against air pressure. Since

the data were captured simultaneously, the plots are expected to exhibit similar trends. It is important to note that

only events with a coincident value of 1 were selected for this analysis (shown in FIG.3.6)

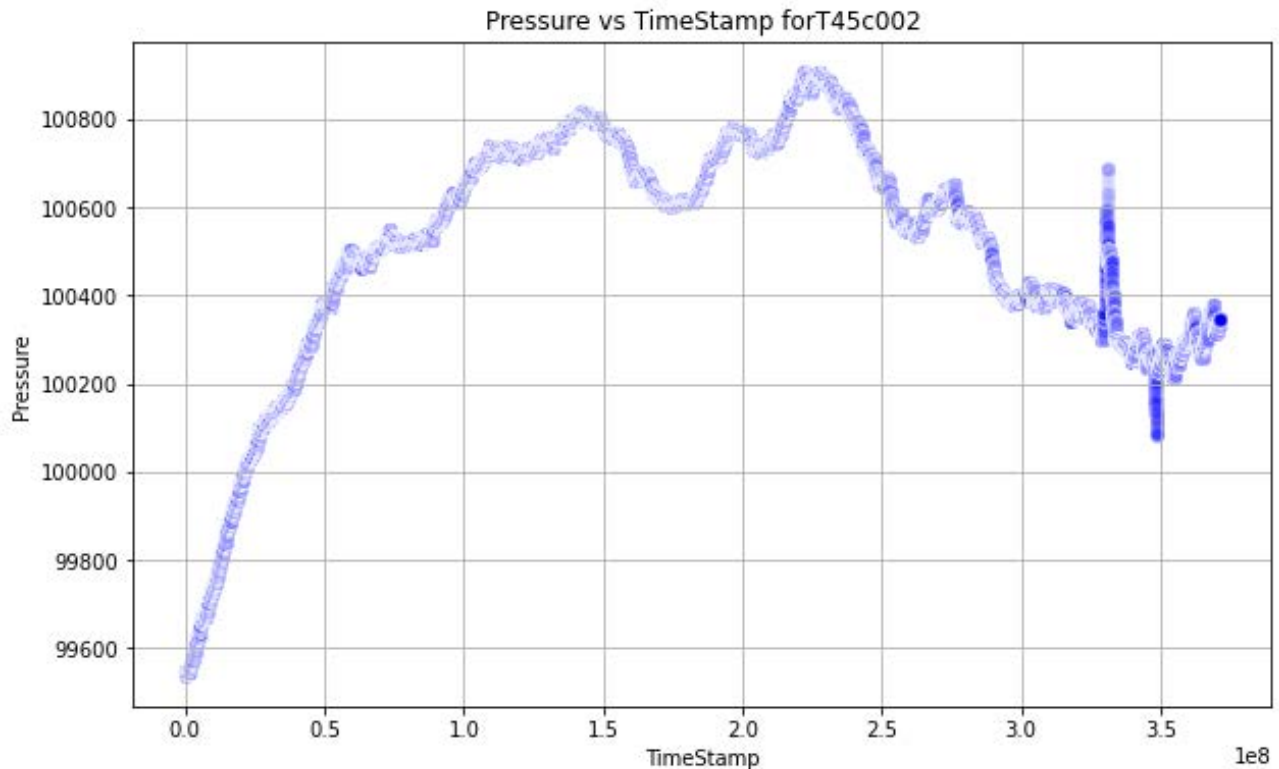


**FIG.3.6 Correlation between TimeStamps and atmospheric pressure over the recorded period**

Next what we do is try to find the relationship between pressure and the rate of muon coincidences. We used the average pressure that we did before, first we got the initial beta value. We define beta as the gradient we took from the graph -- the rate of coincidence 1 per hour over the average rate of coincidence 1 throughout the whole period vs average pressure per hour over average pressure throughout the whole period. each pair of detector we just get one beta value.

The beta value is useful for our calibration of the correlation function between pressure effects and muon coincidences. With the beta value, we deduced the next formula. In this formula we use the measured rate per hour times the beta value and what's more, we make a new comparison between average pressure per hour and standard pressure. The new rate we got is shown in the next paragraph. (shown in FIG.3.7)

We then got a new graph with a more accurate rate value vs average pressure per hour over average pressure throughout the whole period. In these graphs, we can observe that most slopes tend to be horizontal which shows a higher accuracy, and with the observation of each point corresponded pressure ratio. We conclude more about their effects which will be discussed in the next part

Our purpose is to use these sets of data to continue exploring the muon detection between different materials, such as lead and iron. The detected muons through the same piece or the same kind of material should get a similar measured value, according to this we grouped them together and classified which sets of data belong to which kind of material conditions. Here are the grouped results which declare the relationship between materials effects and the rate of detecting muons.(shown in FIG.3.8)

$$Correctedrate = \left(1 - \beta \times \Delta pressure\right) \times Averagenormalisedrate \tag{3.1}$$

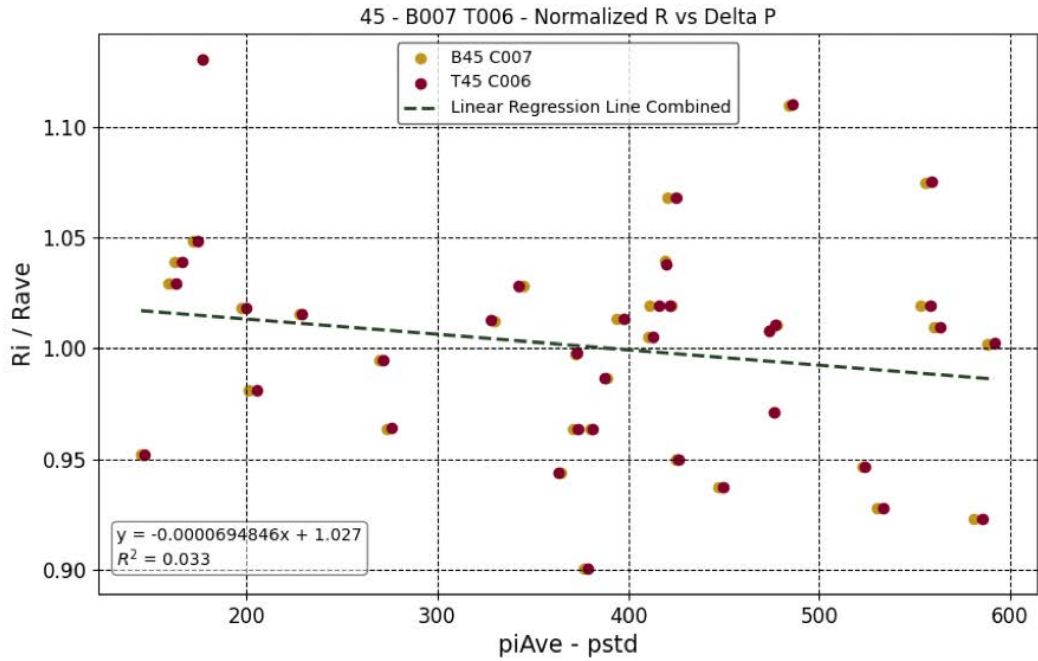


**FIG 3.8** The example of scatter plot and linear best fit line of calibrated rate

we can see that the variations in most points correspond to the relationship between pressure and rate, where points below the standard atmospheric pressure tend to decrease,

while those above tend to increase. We can conclude that even though the rate has been calibrated, it is still not possible to classify them into three groups (three materials).

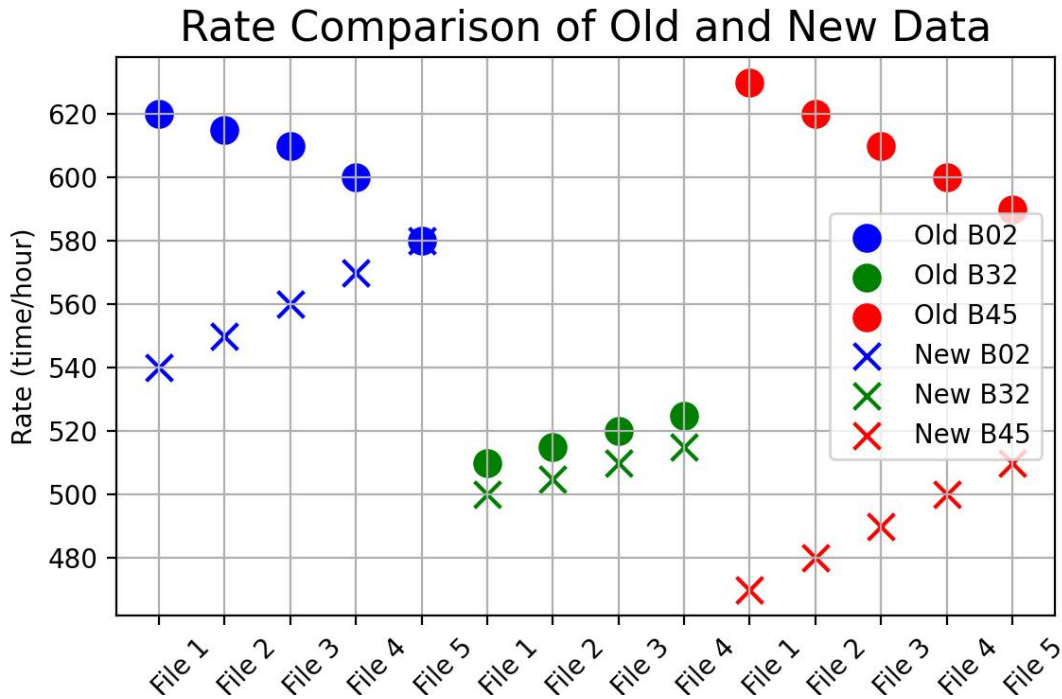


**FIG 3.9**The rate comparison between original data and calibrated data

## 4. Conclusion

In this study, we used raw data collected from the Cosmic Watches to formulate a model for processing raw Cosmic Watch data into standardized and practical data that is capable of identifying double-, and triple-coincident events and distinguishing between environments used across different experiments. To achieve the above, we devised calibrating procedures for the instrumentation and analyzed detected muons' interactions with the experimental environment.

The procedure was applied to identify and account for instrumental errors, such as: discrepancy between Time-Stamp and Air Pressure measurements of identical muon events across different Cosmic Watches. Corrected data was then analyzed through the model to discern double-coincidence events between different combinations of Cosmic Watches. It was also demonstrated that the model is capable of determining the materials that muons pass through before being detected using the correlation between calibrated muon detection rate and material.

However, due to the some limitations of the analysis, future generalization of our procedures must be cautiously conducted for its intended purposes. The correction technique utilized to correct for the pressure sensor error also holds room for error as it took only the pressure difference between one muon detection event. The tolerance for Nor-

malized rate to identify the same muon detection event also varies between different pairs of files as can be seen in Table. I.

Therefore, the correction method for pressure difference requires slight adjustment in the tolerance number for different sets of data. It is proposed that a better procedure should be utilized in the future. The current model introduces a quick calibration model useful for many future experiments involving Cosmic Watches and muon detection. The Cosmic Watches is an affordable introductory instrumentation with great potentiality. With the current model, future scientists can explore an array of coincidence events of different arrangements. For example, it is possible to evaluate the properties of muons by observing triple-coincidence events between a pair of Cosmic Watches stacked together and a separate Cosmic Watch. There should be no coincidence events as Cosmic-ray Muons are incapable of splitting. Nonetheless, it is a property of muon that will be intriguing to observe. The analytic procedure also has the potentiality of investigating Cosmic-ray Muon angular distribution as well as upward-going muons in the momentum range detectable by the Cosmic Watch. The calibration and analytics model will further aid the Cosmic Watches in its many future applications, helping scientists explore the fundamentals of Cosmic-ray muons and perhaps even more.

**Table 4.1 CW45**

File Pairs	Tolerance (%)	$\chi^2$
B7 T6	0.01	0.033
B6 T5	0.0001	0.043
B5 T4	0.001	0.29
B2 T2	0.01	0.035
B1 T1	0.001	0.011

**Table 4.2 CW32**

File Pairs	Tolerance (%)	$\chi^2$
B1 T1	0.001	0.000
B4 T5	0.001	0.019
B5 T4	0.001	0.264
B6 T6	0.001	0.000

Table 4.3 CW02

File Pairs	Tolerance (%)	$\chi^2$
B1 T1	0.01	0.185
B2 T2	0.001	0.097
B5 T3	0.001	0.182
B6 T4	0.001	0.001
B7 T6	0.001	0.004

Table I Three tables for the tolerance and  $\chi^2$  different experiments using CW 02, 32, 45 pairs. Tolerance is adjusted manually.  $\chi^2$  is calculated using Eq.#.  $\chi^2$  poses difficulty in examining the expected values with large datasets similar to data analyzed in the tables above, which is also shown in Fig.3.3

Acknowledgement

Fanyi Shi, Yuwei Niu, Zibing Liu, Yanxin Bian contributed equally to this work and should be considered co-first authors.

References

[1] A. Sharma, "Multi-messenger connection in high-energy neutrino astronomy," *Universe*, vol. 10, no. 8, p. 326, Aug. 2024, doi: 10.3390/universe10080326.

[2] N. Andrés, N. Romanelli, C. Mazelle, L.-J. Chen, J. R. Gruesbeck, and J. R. Espley, "Foreshock Ultra-Low Frequency Waves at Mars: Consequence on the Particle Acceleration Mechanisms at the Martian Bow Shock," Aug. 16, 2024, arXiv: arXiv:2408.09003. Accessed: Aug. 22, 2024. [Online]. Available: <http://arxiv.org/abs/2408.09003>

[3] S. R. Cabo, S. L. S. Gómez, L. Bonavera, M. L. Sanchez, J. D. Santos, and F. J. De Cos, "Magnetic shielding simulation for particle detection," *Eur. Phys. J. Plus*, vol. 138, no. 10, p. 903, Oct. 2023, doi: 10.1140/epjp/s13360-023-04520-1.

[4] S. N. Axani, "The Physics Behind the CosmicWatch Desktop Muon Detectors," Jul. 31, 2019, arXiv: arXiv:1908.00146. Accessed: Aug. 04, 2024. [Online]. Available: <http://arxiv.org/abs/1908.00146>

[5] K. A. Olive, "Review of Particle Physics," *Chinese Phys. C*, vol. 38, no. 9, p. 090001, Aug. 2014, doi: 10.1088/1674-1137/38/9/090001.

[6] "FLUX OF ATMOSPHERIC NEUTRINOS | Annual Reviews." Accessed: Aug. 22, 2024. [Online]. Available: <https://www.annualreviews.org/content/journals/10.1146/annurev-nucl.52.050102.090645>

[7] S. N. Axani, K. Frankiewicz, and J. M. Conrad, "The CosmicWatch Desktop Muon Detector: a self-contained, pocket sized particle detector," *J. Inst.*, vol. 13, no. 03, pp. P03019–P03019, Mar. 2018, doi: 10.1088/1748-0221/13/03/P03019.

[8] "Cosmic rays: particles from outer space," CERN. Accessed: Aug. 22, 2024. [Online]. Available: <https://home.cern/science/physics/cosmic-rays-particles-outer-space>

[9] I. Villa et al., "On the origin of the light yield enhancement in polymeric composite scintillators loaded with dense nanoparticles.".

[10] N. De Angelis, F. Cadoux, C. Husi, M. Kole, and S. Mianowski, "Optimizing the light output of a plastic scintillator and SiPM based detector through optical characterization and simulation: A case study for POLAR-2," Jul. 15, 2024, arXiv: arXiv:2407.10741. Accessed: Aug. 22, 2024. [Online]. Available: <http://arxiv.org/abs/2407.10741>

[11] A. Goshtasbi, R. Zhao, R. Wang, S. Han, W. Ma, and J. Neubauer, "Enhanced Equivalent Circuit Model for High Current Discharge of Lithium-Ion Batteries with Application to Electric Vertical Takeoff and Landing Aircraft," Aug. 15, 2024, arXiv: arXiv:2408.07926. Accessed: Aug. 22, 2024. [Online]. Available: <http://arxiv.org/abs/2408.07926>

[12] C. Yu, Q. Xu, and J. Zhang, "Recent advances in InGaAs/InP single-photon detectors," Aug. 13, 2024, arXiv: arXiv:2408.06921. Accessed: Aug. 22, 2024. [Online]. Available: <http://arxiv.org/abs/2408.06921>

[13] W. Fang et al., "Obstacle-Aware Length-Matching Routing for Any-Direction Traces in Printed Circuit Board," Jul. 27, 2024, arXiv: arXiv:2407.19195. Accessed: Aug. 22, 2024. [Online]. Available: <http://arxiv.org/abs/2407.19195>

[14] M. L. McHugh, "The Chi-square test of independence," *Biochem Med (Zagreb)*, vol. 23, no. 2, pp. 143–149, Jun. 2013, doi: 10.11613/BM.2013.018.